10.1109/ULTSYM.2009.0561

Improved estimation of parameters of the homodyned K distribution

David Hruska, Roberto Lavarello, William D. O'Brien Jr., and Michael L. Oelze
Bioacoustics Research Laboratory
Department of Electrical and Computer Engineering
University of Illinois at Urbana-Champaign
Urbana, IL 61801
Email: oelze@illinois.edu

Abstract— The amplitude distribution of the envelope of backscattered ultrasound depends on tissue microstructure. By fitting measured envelope data to a model, parameters can be estimated to describe properties of underlying tissue. The homodyned K distribution is a general model that encompasses the scattering situations modeled by the Rice, Rayleigh, and K distributions. However, parameter estimation for the homodyned K distribution is not straightforward because the model is analytically complex. Furthermore, effects of frequency-dependent attenuation on parameter estimates need to be assessed. An improved parameter estimation algorithm was developed to quickly and accurately estimate parameters of the homodyned K distribution, i.e., the μ (effective number of scatterers per resolution cell) and *k* (ratio of coherent to diffuse energy) parameters. Parameter estimates were found by fitting estimates of SNR, skewness, and kurtosis of fractional-order moments of the envelope with theoretical values predicted by the homodyned K distribution. The effects of frequency dependent attenuation were approximated by assuming a Gaussian pulse to determine the shift in center frequency of the pulse and hence change in volume of the resolution cell. Computational phantoms were created with varying attenuation coefficients and scanned using a simulated f/4 transducer with a center frequency of 10 MHz. An average of two scatterers per resolution cell (based on the phantoms with no attenuation) was used. The new estimation algorithm was tested and compared with an existing algorithm (based on the even moments of the homodyned K distribution). The new estimation algorithm was found to produce estimates with lower bias and variance. For example, for $\mu = 2$ and k ranging from 0 to 2 in steps of 0.1, the average variance in the μ parameter estimates was 0.067 for the new algorithm and 0.42 for existing algorithm. For the k parameter estimates, the average variance was 0.0069 for the new algorithm and 0.048 for the old algorithm. In the simulations with no attenuation, the μ parameter estimate was 2.53 ± 0.18. In the phantoms with a linear attenuation coefficient of 0.5 $dB \cdot MHz^{-1} \cdot cm^{-1}$, the estimate was 4.64 ± 0.54. This compared well with the predicted μ value of 4.98.

Backscatter; Envelope Statistic;Tissue Characterization

This work was supported in part by the National Institutes of Health Grants CA111289 and EB008992.

I. Introduction

Statistical analysis of the envelope of backscattered ultrasound has been used to characterize tissues and may be useful for improving the diagnostic capabilities of ultrasound. Shankar *et al.* [1] demonstrated the potential efficacy of envelope-based statistics in distinguishing benign and malignant breast masses. Hao *et al.* [2] used the homodyned K distribution to differentiate normal and abnormal myocardium. Sommer *et al.* [3] observed statistically significant differences in the mean and variance of the amplitude distribution of the envelope signal from normal and cirrhotic livers.

A number of different models for the amplitude distribution of the envelope signal have been proposed over the past few decades. The homodyned K distribution is a particularly versatile but analytically complex model. Because of this complexity, its use has been somewhat limited and other, more analytically tractable models such as the Nakagami distribution, Weibull distribution, Rician, and generalized gamma distribution have been used instead. However, by applying an improved parameter estimation algorithm, estimates of parameters of the homodyned K distribution can be obtained in a relatively simple way.

Until recently, parameter estimation based on fractional order moments was rarely used with the homodyned K distribution but more often with the more tractable K distribution. Martín-Fernández *et al.* [4] originally developed a mathematically tractable implementation of a parameter estimation algorithm for the homodyned K distribution based on arbitrary fractional order moments. The estimation algorithm presented here is an extension of this original idea.

II. Methods

A. Homodyned K Distribution

The homodyned K distribution was first introduced by Jakeman [5]. Besides incorporating the capability of the K distribution to model situations with low effective scatterer number densities, the homodyned K distribution can also model situations where a coherent signal component exists due to periodically located scatterers [6]. This makes the homodyned K distribution a versatile option, but also complicated. The pdf of the homodyned K distribution does not have a closed-form expression; however, it can be expressed in terms of an improper integral as [7]

$$p_A(A) = A\int_0^\infty xJ_0(sx)J_0(Ax)\left(1+\frac{x^2\sigma^2}{2\mu}\right)^{-\mu} dx \qquad (1)$$

where $J_0(\cdot)$ is the zeroth order Bessel function of the first kind, s^2 is the coherent signal energy, σ^2 is the diffuse signal energy, and μ is the same parameter as defined in the K distribution. The derived parameter $k = s/\sigma$ is the ratio of the coherent to diffuse signal and can be used to describe the level of structure or periodicity in scatterer locations.

B. Parameter Estimation

Martín-Fernández *et al.* [4] observed that the SNR of arbitrary moments of the echo envelope predicted by the homodyned K distribution was a function of only the two independent parameters (the k and μ parameters). This allowed an estimator to be implemented based on crossing level curves derived using different fractional-order moments in the Cartesian plane of the parameters (k, μ). By first calculating theoretical values for the SNR for a range of parameter values, an efficient estimator was developed.

Moments of arbitrary order ν of the homodyned K distribution can be expressed as [4]

$$E\left[A^\nu\right] = \int_0^\infty \left(\frac{2\sigma^2}{\mu}\right)^{\frac{\nu}{2}} \frac{\Gamma\left(1+\frac{\nu}{2}\right)x^{\frac{\nu}{2}+\mu-1}}{\Gamma(\mu)e^x} {}_1F_1\left(\frac{-\nu}{2};1;\frac{-\mu s^2}{2\sigma^2 x}\right)dx \qquad (2)$$

where ${}_1F_1(a;b;x)$ is the confluent hypergeometric function of the first kind. By substituting $k = s/\sigma$ in the argument of the hypergeometric function, defining the improper integral as a function of three variables,

$$I(k,\mu,\nu) = \int_0^\infty \frac{\Gamma\left(1+\frac{\nu}{2}\right)x^{\frac{\nu}{2}+\mu-1}}{\Gamma(\mu)e^x} {}_1F_1\left(\frac{-\nu}{2};1;\frac{-\mu s^2}{2\sigma^2 x}\right)dx \qquad (3)$$

and pulling constants out of the integral, (2) can be written as

$$E\left[A^\nu\right] = \left(\frac{2\sigma^2}{\mu}\right)^{\frac{\nu}{2}} I(k,\mu,\nu)\,. \qquad (4)$$

Performing the integration in (3) and simplifying,

$$I(k,\mu,\nu) = \frac{\Gamma(1+\nu/2)}{\Gamma(\mu)}\left[\Gamma(\eta)\,{}_1F_2\left(-\frac{\nu}{2};1,1-\eta;\frac{k^2\mu}{2}\right) - \frac{\Gamma(\mu)\pi\csc(\eta\pi)}{\Gamma(-\nu/2)\Gamma^2(1+\eta)}\left(\frac{k^2\mu}{2}\right)^{\eta} {}_1F_2\left(\mu;1+\eta,1+\eta;\frac{k^2\mu}{2}\right)\right] \qquad (5)$$

where ${}_1F_2(a;b,c;x)$ is a hypergeometric function and, for convenience, the definition

$$\eta = \mu + \frac{\nu}{2} \qquad (6)$$

is used. Thus, moments of the homodyned K distribution of arbitrary order can be evaluated numerically in a relatively simple way using (3) and (4).

This original idea was extended to calculate the SNR algebraically. Furthermore, the skewness and kurtosis functions have been included in the proposed algorithm to increase the sensitivity to larger scatterer number densities (i.e., up to 10 scatterers per resolution cell). The SNR, skewness, and kurtosis of samples of the echo envelope of order ν can be expressed as [8], [9]

$$R_\nu = \frac{E[A^\nu]}{\left(E[A^{2\nu}] - E^2[A^\nu]\right)^{1/2}} \qquad (7)$$

$$S_\nu = \frac{E[A^{3\nu}] - 3E[A^\nu]E[A^{2\nu}] + 2E^3[A^\nu]}{\left(E[A^{2\nu}] - E^2[A^\nu]\right)^{3/2}} \qquad (8)$$

$$K_\nu = \frac{E[A^{4\nu}] - 4E[A^\nu]E[A^{3\nu}] + 6E[A^{2\nu}]E^2[A^\nu] - 3E^4[A^\nu]}{\left(E[A^{2\nu}] - E^2[A^\nu]\right)^2}\,. \qquad (9)$$

Following [4], the subscript ν indicates the dependence on the moment order ν. By relating to (6), these three equations are functions of the μ and k parameters only. Parameter estimation is performed by equating estimates of SNR, skewness, and kurtosis from the envelope signal with theoretical values predicted by the homodyned K distribution. By using these functions, parameter estimates can be obtained from level curves in the two-dimensional parameter space [4].

Parameter estimates were obtained by finding the point in (k, μ) space where the L2-norm of the distances from the level curves was minimized. Fig. 1 shows an example using three level curves. The generally vertical orientation in the curves derived from skewness and kurtosis suggests that the algorithm is more sensitive to changes in the μ parameter than the algorithm based on SNR alone and will result in improved variance of estimates over SNR curves alone.

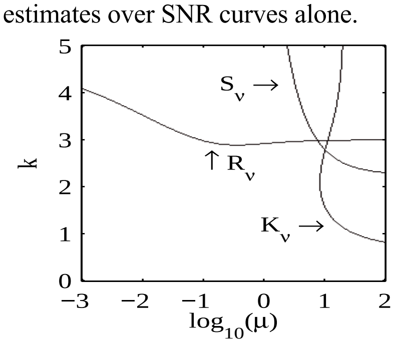

Fig. 1. Level curves based on moment order ν = 1. Intended parameters: k = 3, $\log_{10}(\mu)$ = 1.

Although true optimal moment orders may not exist, the choice of moment order may affect the performance of the estimation algorithm. Therefore, an effort was made to select moments that were in some sense optimal. The SNR, skewness, and kurtosis were sampled on a 501 × 501 point grid with k uniformly spaced on the interval [0, 5] and $\log_{10}(\mu)$ uniformly spaced on the interval [-3, 2]. These functions were sampled for moments $\nu \in \{0.02, 0.04, \ldots, 1.00\}$.

The goal of the optimization was to select two moment orders such that the six intersecting level curves (SNR, skewness, and kurtosis for each of the two moment orders) would represent a system as well-conditioned as possible for the largest possible range of parameter values. Geometrically, when level curves are nearly parallel at the point of intersection, the system is ill-conditioned as the intersection point is sensitive to small perturbations in the input data. Conversely, level curves that intersect perpendicularly correspond to a well-conditioned system. Based on these observations, moment orders were selected to produce the best possible conditioning.

The gradients of the SNR, skewness, and kurtosis functions were evaluated numerically at each point where they were sampled. From the gradient, the angle of the level curve passing through each point (k_1, μ_1) was determined as

$$\theta = \arctan\left(-\frac{g_\mu\left(k_1,\mu_1\right)}{g_k\left(k_1,\mu_1\right)}\right) \qquad (10)$$

where g_μ and g_k are the components of the gradient in the μ and k directions, respectively. Considering two moments at a time, the sum of the angles between all pairs of level curves was calculated for each point where the functions were sampled. An average value was obtained over the entire (k, μ) space examined. The pair of moments that maximized this sum was selected for estimation, i.e., the pair of moments that resulted in level curves less likely to be parallel at their intersection over the range of μ and k parameters examined. The "optimal" pair of moments was found to be $v \in \{0.72, 0.88\}$. These moments will be used throughout the rest of this work.

The algorithm was tested by constructing computational phantoms with different number densities and with different ratios of randomly spaced scatterers versus periodically spaced scatterers. Estimates of the μ and k parameters were obtained using the new algorithm and an even moments method and compared. The bias and variance of estimates using both methods were calculated for comparison.

C. *Quantifying the Effects of Attenuation*

Assuming an attenuation coefficient that is linearly increasing with frequency, the frequency-dependent attenuation results in higher frequencies being attenuated more rapidly with depth than lower frequencies. This can produce a shift in the center frequency of the imaging pulse. Assuming a Gaussian pulse, the shift in center frequency, Δf, is given by

$$\Delta f = f' - f_0 = \frac{-\alpha_0 x\left(2.66 f_0 B\right)^2}{4\pi^2} \qquad (11)$$

where f' and f_0 are the center frequencies of the pulse with and without attenuation, respectively.

Approximating the resolution cell as a cylinder and assuming that the fractional bandwidth is unchanged by attenuation, the ratio of the volume of the resolution cell in the presence of attenuation (V') to the volume of the resolution cell without attenuation (V) is given by

$$\frac{V'}{V} = \left(\frac{f_0}{f'}\right)^3. \qquad (12)$$

Combining Eqs. (11) and (12) yields

$$\frac{V'}{V} = \left(\frac{4\pi^2}{4\pi^2 - (2.66)^2 \alpha_0 f_0 x B^2}\right)^3. \qquad (13)$$

The estimated scatterer number density (scatterers per resolution cell) should increase according to the increase in the volume of the resolution cell predicted by (13).

Computational phantoms were used to verify the predictions from (13). Ten independent phantoms were generated for each attenuation coefficient value used. Each phantom was scanned using two imaging pulses with different fractional bandwidths. Each resulting image was analyzed using the new envelope statistics algorithm.

III. Results

A. *Algorithm Performance*

Figures 2 and 3 show the relative bias and variance of estimates using the traditional even moments method and the new algorithm, respectively. The new estimation algorithm was found to produce estimates with lower bias and variance. For example, for $\mu = 2$ and k ranging from 0 to 2 in steps of 0.1, the average variance in the μ parameter estimates was 0.067 for the new algorithm and 0.42 for existing algorithm. For the k parameter estimates, the average variance was 0.0069 for the new algorithm and 0.048 for the old algorithm.

B. *Quantifying the Effects of Attenuation*

The results shown in Fig. 4 were obtained by averaging the estimated scatterer number density from the 10 independent phantoms used for each attenuation coefficient. Both the theoretical and estimated scatterer number densities varied substantially as the attenuation coefficient changed when the phantoms were imaged using a pulse with 50% fractional bandwidth (Fig. 4a). By reducing the fractional bandwidth to 25%, this variation was reduced substantially (Fig. 4b). These results are consistent with previously reported measurements of physical phantoms [10]. In the simulations with no attenuation, the μ parameter estimate was 2.53±0.18. In the phantoms with a linear attenuation coefficient of 0.5 $dB \cdot MHz^{-1} \cdot cm^{-1}$, the estimate was 4.64±0.54. This compared well with the predicted μ value of 4.98.

Note that the reduction in fractional bandwidth requires the use of a longer imaging pulse, reducing the axial resolution of the resulting image. Also, this increases the volume of the resolution cell in the absence of attenuation. When the scatterer number density is large, it is desirable to reduce the volume of the resolution cell to avoid exceeding the Rayleigh limit of about 10 scatterers per resolution cell beyond which scatterer number density estimation becomes unreliable.

IV. Conclusions

A new algorithm was developed to estimate scattering parameters based on the homodyned K distribution and the backscattered envelope. The new algorithm was based on calculating the SNR, skewness, and kurtosis using fractional order moments with optimal moments found to be 0.72 and 0.88. The new algorithm was evaluated using simulated phantoms and compared with estimates using an even moments method. Improved bias and variance of estimates was obtained using the new algorithm. The effects of frequency-dependent attenuation were evaluated and found to result in an increase in the estimated scatterers per resolution cell. Therefore, to make estimation of the μ parameter system independent, it is necessary to account for the frequency-dependent attenuation on the size of the resolution cell.

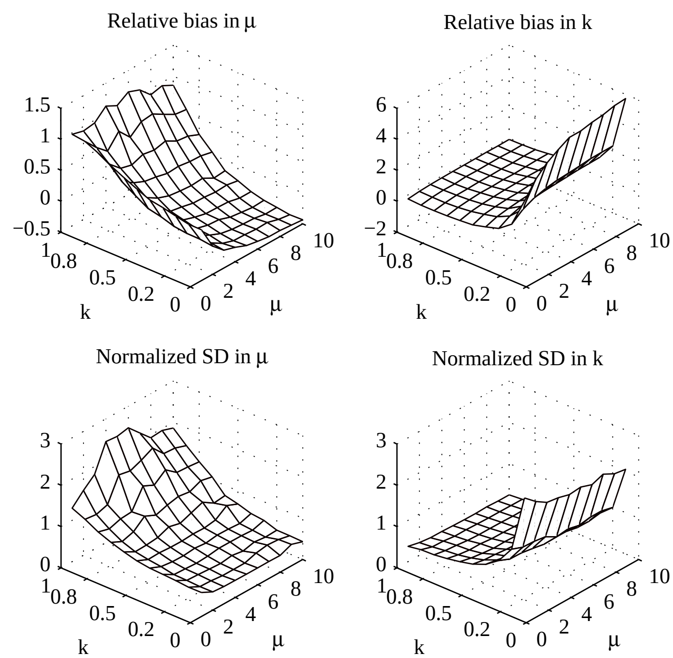

Fig. 2. Relative bias and standard deviation (SD) of model parameter estimates versus the model parameters (even moments algorithm).

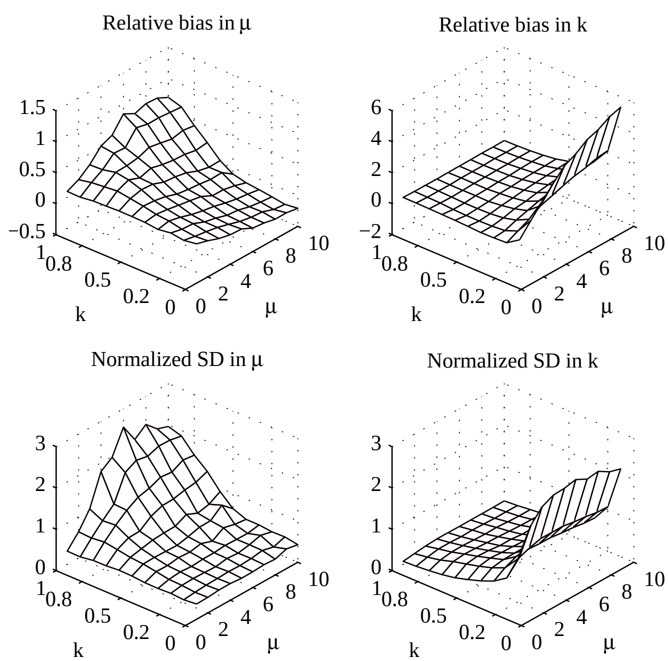

Fig. 3. Relative bias and normalized SD of model parameter estimates versus the model parameters (new algorithm).

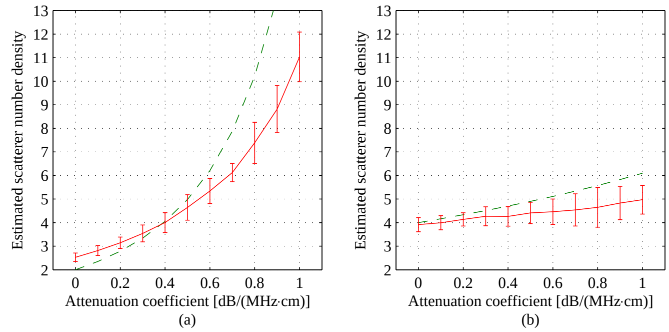

Fig. 4 Estimated scatterer number density for simulated phantoms versus attenuation coefficient using a pulse with (a) 50% fractional bandwidth and (b) 25% fractional bandwidth. The error bars are two standard deviations. Ideal estimates are the green dashed line.

ACKNOWLEDGMENTS

The authors would like to thank Jose Sanchez for his useful discussions regarding this work.

REFERENCES

[1] P. M. Shankar, V. A. Dumane, T. George, C. W. Piccoli, J. M. Reid, F. Forsberg, and B. B. Goldberg, "Classification of breast masses in ultrasonic B scans using Nakagami and K distributions," *Physics Med Biol*, vol. 48, pp. 2229-2240, 2003.

[2] X. Hao, C. J. Bruce, C. Pislaru, and J. F. Greenleaf, "Characterization of reperfused infarcted myocardium from high-frequency intracardiac ultrasound imaging using homodyned K distribution," *IEEE Trans on Ultrason, Ferro, Freq Contr*, vol. 49, pp. 1530-1542, 2002.

[3] F. G. Sommer, L. F. Joynt, B. A. Carroll, and A. Macovski, "Ultrasonic characterization of abdominal tissues via digital analysis of backscattered waveforms," *Radiology*, vol. 141, pp. 811-817, 1981.

[4] M. Martín-Fernández, R. Cárdenes, and C. Alberola-López, "Parameter estimation of the homodyned K distribution based on signal to noise ratio," *Proc IEEE Ultrasonics Symposium*, pp. 158-161, 2007.

[5] E. Jakeman, "On the statistics of K distributed noise," *J Physics A: Mathemat General*, vol. 13, pp. 31-48, 1980.

[6] R. Smolíková, "Neural and statistical modeling of ultrasound backscatter," Ph.D. dissertation, University of Louisville, Louisville, KY, 2002.

[7] V. Dutt and J. F. Greenleaf, "Ultrasound echo envelope analysis using a homodyned K distribution signal model," *Ultrasonic Imaging*, vol. 16, pp. 265 287, 1994.

[8] R. W. Prager, A. H. Gee, G. M. Treece, and L. H. Berman, "Analysis of speckle in ultrasound images using fractional order statistics and the homodyned k distribution," *Ultrasonics*, vol. 40, pp. 133-137, 2002.

[9] M. G. Bulmer, *Princ Statistics*. Cambridge, MA: The M.I.T. Press, 1965.

[10] J. A. Zagzebski, J.-F. Chen, F. Doug, and T. Wilson, "Intervening attenuation affects first-order statistical properties of ultrasound echo signals," *IEEE Trans on Ultrason, Ferro, Freq Contr*, vol. 46, pp. 35-40, 1999.